Naghipour, D, Taghavi, K, Jaafari, J, Hashim, KS, Javan Mahjoub Doust, F and Mahjoub Doust, MJ

Evaluation of the efficacy of Fe2O3 magnetised kaolin: Simultaneous removal of ceftriaxone and cefixime from aqueous media

https://researchonline.ljmu.ac.uk/id/eprint/17907/

Article

Citation (please note it is advisable to refer to the publisher's version if you intend to cite from this work)

Naghipour, D, Taghavi, K, Jaafari, J, Hashim, KS ORCID logoORCID: https://orcid.org/0000-0001-9623-4060, Javan Mahjoub Doust, F and Mahjoub Doust, MJ (2022) Evaluation of the efficacy of Fe2O3 magnetised kaolin: Simultaneous removal of ceftriaxone and cefixime from aqueous

Evaluation of the efficacy of Fe_2O_3 magnetised kaolin: Simultaneous removal of ceftriaxone and cefixime from aqueous media

Dariush Naghipour[1], Kamran Taghavi[1], Jalil Jaafari[2], Khalid S. Hashim[3], Fatemeh Javan Mahjoub Doust[1], Mehri Javan Mahjoub Doust[1*]

[1]Department of Environmental Health Engineering, School of Health, Guilan University of Medical Sciences, Rasht, Iran; dnaghipour@yahoo.com (D. Naghipour), user37@gums.ac.ir (K. Taghavi), javan.m.f@gmail.com (F.J. Mahjoub Doust)

[2]Department of Environmental Health Engineering, School of Health, Tehran University of Medical Sciences, Tehran, Iran; Jalil.Jaafari@yahoo.com

[3]Built Environment and Sustainable Technologies (BEST) Research Institute, Liverpool John Moores University, Liverpool L3 3AF, UK; k.s.hashim@ljmu.ac.uk

***Corresponding author: mahmehrijavan@gmail.com**

Abstract

Traces of antibiotics in domestic and industrial effluents have toxic effects on human health and the surrounding plants and animals, besides their potential to increase antibiotic resistance of microorganisms. Therefore, this study aims to develop a new adsorbent made from Kaolin magnetised with Fe_3O_4 (Kaolin-Fe_3O_4) nanocomposites and apply it to remove ceftriaxone and Cefixime from aqueous solutions. The efficiency of the new adsorbent in removing ceftriaxone and Cefixime from solutions was studied under different adsorbent doses, antibiotic concentrations, solution pH values, and contact times. The results indicated the best ceftriaxone and Cefixime removal was attained at pH of 5 and 3, respectively, while the best antibiotic concentration, contact time, and the adsorbent dose were 20 mg/L, 60 min, and 0.4 g/250 cc, respectively. It was noticed the adsorption was improved at low temperatures ((25℃ for ceftriaxone and 35℃ for Cefixime). Five types of isotherms were used to match the equilibrium data, including Langmuir, Freundlich, Temkin, Redlich-Peterson, and Sips. Equilibrium data were also matched with pseudo-first and second-order kinetics, Elovich, and intraparticle diffusion. Freundlich and Sips isotherm models were more consistent with equilibrium data. The positive results of Gibbs free energy and the negative enthalpy obtained from thermodynamic parameters indicate that the adsorption process is spontaneous and the adsorption process is exothermic. In light of the obtained results, the Kaolin-Fe_3O_4

nanocomposites could be considered an effective and inexpensive adsorbent for removing antibiotics from aqueous solutions.

Keywords: Kaolin-Fe_3O_4 nanocomposite, Ceftriaxone, Cefixime, Thermodynamics

Introduction:

Among water-consuming units, hospitals are usually the most consumed units, which are converted into wastewater after consumption (1). The common components of hospital wastewater can be listed as biodegradable organic matter, minerals (soluble, colloidal, and suspended), Toxic metals (mercury, lead, etc.), detergents, disinfectants (chlorine, hydrogen peroxide, etc.), microbial pathogens (bacteria, viruses), hazardous chemical compounds, drug compounds (antibiotics, drugs, Hormone drugs, etc.) and radioactive isotopes (2, 3).

The term "antibiotic" is composed of the two words, i.e., anti and biosis, which account for about 15% of all drugs (4). Their presence in aquatic environments is a significant concern associated with ecosystem damage (5). Most antibiotics are partially metabolised in the body, and the rest, about 30-90%, are excreted into the sewage system without being metabolised (6, 7). Low concentrations of antibiotics reduce sperm count, increase breast and prostate cancer and lead to carcinogenicity and mutagenicity, DNA damage, and lymphocyte damage (8).

Antibiotics are chemical compounds that inhibit the growth of microorganisms, often have a microbial origin, and may be semi-artificial or completely artificial (9). One of the most important antibiotics used to treat infections is ceftriaxone and Cefixime. Ceftriaxone is a third-generation cephalosporin antibiotic and, like other third-generation cephalosporins, has a wide range of activity against gram-positive and gram-negative bacteria (10). Cephalosporin antibiotics are often used (in combination with an aminoglycoside or macrolide antibiotics) to treat pneumonia. These drugs are also selected to treat bacterial meningitis and are commonly used in paediatrics for febrile children. They are also used in treating leptospirosis, lymphatic disease, and gonorrhoea, besides employing it as a routine prophylactic antibiotic in orthopaedic surgery (11).

The relatively low Henry's law constant of these antibiotics indicates that these compounds are difficult to destroy by evaporation. The high solubility and low water-octanol separation coefficient of these compounds show their hydrophilic properties (12). Due to their widespread use and higher absorption capacity, these antibiotics are found in various environmental matrices, including surface water, groundwater, municipal wastewater, and sedimented soil. Conventional municipal wastewater treatment plants do not have the ability to completely remove these micro-pollutants (13, 14). The removal efficiency of antibiotics in wastewater treatment plants is reported to be from 12% to 43%, which is very low (15). Given the dangers of the presence of these antibiotics in the ecosystem, there is a need to develop effective and efficient treatment processes to adsorb these compounds from contaminated water and minimise their environmental hazards (16, 17).

Conventional water and wastewater treatment processes are not designed to remove small amounts of chemicals such as antibiotics (18). Due to the increasing number of reports of these compounds in the environment, developing effective, efficient, and cost-effective treatment processes is even more important to remove these compounds from polluted water and minimise their environmental hazards (19, 20). Several processes can be used to remove antibiotics from water sources. These processes include advanced oxidation, ion exchange, activated carbon adsorption, reverse osmosis, and biological treatment (21, 22). However, biological treatment is not very effective in removing antibiotics because antibiotics eliminate microorganisms that are effective in treatment (22, 23).

One of the most important processes is the adsorption of pollutants, which is widely used due to the lack of expertise and its simple design. The most important adsorbent used in water and wastewater treatment is activated carbon. Although the use of carbon nanotubes and nanoparticles in water treatment has dramatically increased in recent years, these adsorbents are expensive, and their regeneration is associated with problems (24). So in recent years, researchers have been looking for inexpensive adsorbents to reduce treatment costs.

Kaolin is one of the most common silicate mineral compounds with a chemical formula of $Al_2Si_2O_5(OH)_4$. It is a layered chemical-silicate mineral compound with a quadrilateral sheet attached to an octahedral sheet by oxygen atoms (25). The successive layers are held together by hydrogen bonds between the silica and alumina layers. The quadrilateral sheet carries a permanent negative charge due to the substitution of Al^{+3} with Si^{+4} and leaving a negative charge for each replacement. Kaolin is a soft and white compound used in ceramic, medical, paper making, cosmetic, and food industries. Kaolin is abundantly found in Iran (26). The average annual production of this widely used mineral in Iran is estimated at 500,000 tons (27). Therefore, it has many applications in terms of cheapness and suitability for environmental work (25). Kaolin has been used to remove colourful effluents and heavy metals, which has high efficiency (27, 28).

Nonetheless, one of the problems with adsorbents is that they are disposable or need regeneration, and they are very difficult to regenerate. Therefore, this problem can be solved and minimised by magnetising the adsorbent (29). Many efforts have been made during the last decades to find high-efficient and highly recyclable magnetic attractions. Fe_2O_3 is used more than other iron compounds for different reasons, such as moderate magnetic saturation, high chemical stability, and strong anisotropy (30).

This study has performed the removal of ceftriaxone and Cefixime antibiotics by a cost-effective adsorbent(magnetised kaolin adsorbent) Then, the effect of various parameters such as effluent pH, adsorbent concentration, initial concentration of the antibiotic, temperature, and time have been studied. Finally, isotherms, kinetics, and thermodynamics on magnetised Kaolin were investigated, and the results were compared with other sources.

Materials and methods

The present study was an experimental-applied study in which the performance of Fe_2O_3/kaolin nanocomposites in the adsorption of ceftriaxone and Cefixime antibiotics was investigated. In the current work, all laboratory materials, including ceftriaxone and Cefixime, hydrochloric acid, divalent, sodium hydroxide, and divalent and trivalent iron, were prepared by Merck Company. Kaolin powder was prepared from the ideal Trades Men Company, Qazvin. A magnet with a magnetic intensity of 1.3 Tesla was used to separate the adsorbent from the solution magnetically. Deionised water was used to prepare all test solutions. In addition, 0.1 M hydrochloric acid and sodium hydroxide were used to adjust the pH of the solution.

Synthesis of Fe_2O_3/kaolin nanocomposites

The study of Guo et al. was employed for preparing Fe_2O_3/kaolin nanocomposites (31). Kaolin was first prepared for synthesising nanocomposites; Kaolin was first prepared; accordingly, Kaolin was rinsed with deionised water, dried in an oven at 103°C for 3 hours, and sieved in ASTM 50 mesh size. The synthesis of Fe_2O_3-kaolin nanocomposite was done as follows: iron chloride (II) and iron chloride (III) in a 2: 1 stoichiometric ratio and kaolin powder in a 1: 1 stoichiometric ratio were mixed with 80 ml of 96% ethanol and 20 ml of deionised water. Reflux was then performed at 80°C for one hour. Then, 20 ml of ammonium hydroxide was added and the reflux was continued for another two hrs to obtain a bituminous colour solution. After washing with deionised water and ethanol, the particles were separated by a magnet and dried at room temperature (32). By heating the sample at a temperature above 150 °C at 60 min, the colour change from bitumen to reddish-brown indicates the formation of γ-Fe_2O_3, which was confirmed by X-ray analysis. It should be noted that the synthesis of γ-Fe_2O_3 without the presence of Kaolin was first performed to ensure its correctness, and then the synthesis of the nanocomposite was performed. The determination of the type of nanoparticle was done by X-ray analysis (XRD, PW1730 model). The particle size was done using scanning energy microscope analysis (FESEM, MIRA III model). Fourier transform infrared spectroscopy (FT –IR, AVATAR model) was also performed on powdered samples.

Adsorption tests

First, the stock solution of antibiotics was prepared from Cefixime and ceftriaxone powder, so that 0.25 g of commercial Cefixime and ceftriaxone powder with 98% purity was dissolved in 250 cc of distilled water in a volumetric flask. The stock solution of 1000 mg/L was obtained. To conduct this research, determining the optimal test conditions were first done based on the effect of changes in the studied parameters, including nanocomposite dose (0.1, 0. 2, 0.3, 0.4, 0.5, and 0.6 gr), pH (3, 5, 7, 9, and 11), contact time (0 to 120 min), initial contaminant concentration (20, 40, 80, and 120 mg/L) and temperature (25-55˚C) on the removal efficiency of Cefixime and ceftriaxone in the tested system. For example, to determine the optimal pH value, a specific and constant amount of adsorbent and antibiotic concentration was in all 5 balloons, and at a specific contact time, the amount of removal percentage was evaluated; the only difference among these 5 balloons was the pH value, which was varied from 3 to 11. The magnet was used to separate and reuse the adsorbent so that after each use, nanoparticles were collected using the magnet and the final concentration of antibiotics in the effluent was measured using the device spectrophotometer (Model: DR 5000) at a wavelength of 293 for ceftriaxone and 295 for Cefixime. Finally, the removal efficiency and adsorption capacity were calculated according to Eqs. 1 and 2 (33).

$$\% R = \frac{(C_0 - C_e)}{C_0} \times V \qquad (1)$$

$$q_e = \frac{C_0 - C_e}{M} \times V \qquad (2)$$

where C_0 and C_e are the initial concentration and the equilibrium concentration of the antibiotic (mg/L), m is the mass of the nanocomposite used (gr), and V is the volume of solution (L).

Results and discussion

Characterisation of adsorbent

The SEM images of the Kaolin and the Fe_2O_3–Kaolin were publicised in Figure 1a-b. As depicted in Figure 1a, the characteristic structure of hexagonal platelets with a thickness range of 50-–100 mm was approved for the Kaolin. Through the thermal treatment, a dehydroxylation process occurs; this can diminish the number of hydrogen groups bonding between the Al–O octahedron sheet and Si–O tetrahedron sheet, which consequently leads to more unrestricted movement of OH- in the sheet interspace (31). Thus, in the thermal treatment, drastic modification is not observed in the morphology, compared with Figure 1a, and only a tendency of aggregation was observed after calcination (Figure 1b).

Measuring the phase behaviour of neat Kaolin, Fe_2O_3–Kaolin, and Fe_2O_3 was carried out by an X-ray diffractometer (Figure 2a-c). The presence of characteristic peaks detected in neat Kaolin and Fe_2O_3–Kaolin were related to kaolinite ($2\theta = 12.3^{\circ}$, 21.2°, 25.8◦) and muscovite ($2 = 17.88^{\circ}$, 27.6°); it is indicative of the stability of Al–O octahedron structure and less of losses in layered crystallinity structure at high temperature (31). Moreover, according to Figures 2b and c (Fe-related species), the diffraction peaks at 35.61° and 54.3° were clearly observed, which are assigned to Fe_2O_3; this approves the successful modification of the neat Kaolin by Fe species.

The FT-IR was another analysis used in this study as another tool to confirm the stability of the Kaolin, Fe_2O_3 and Fe_2O_3–Kaolin. According to Figure 3b, the infrared spectrum (FTIR) of the Fe_2O_3 nanoparticles was in the range of 400- 4000 cm^{-1} wavenumber. The large broadband at 3435 cm^{-1} is ascribed to the O-H stretching vibration in O$\overline{\text{H-}}$ groups. The absorption peaks were around 1635 cm^{-1} due to the symmetric and asymmetric bending vibration of C=O. The strong band below 700 cm^{-1} is assigned Fe-O stretching mode. Also, as portrayed in Figure 3c, peaks at 3698.6, 3620.6, 3435, 1634, 1033.9, 912.9, 636.6 and 540.7 cm^{-1} were the FT-IR spectrum of the Fe_2O_3–Kaolin; these peaks were related to characteristics of Kaolin. Bands at 3435 and 1634 cm^{-1} were correspondents to OH-stretching, and bands at 3698.6, 3620, and 912.6 cm^{-1} were related to Al–OH stretching and C=O (34). In 1500–500 cm^{-1}, which was the lower frequency region of the spectra, bands at 1033.9 and 912.9 cm^{-1} were related to Si–O stretching vibration and bands at 636.6 and 540.7 cm^{-1} were correspondent to Si–O–Al stretching vibration. The functional groups of Fe_2O_3–Kaolin were also observed in Kaolin (Figure 3a) and Fe_2O_3 (Figure 3b). This indicates that the nanocomposite is well magnetised and retains its properties.

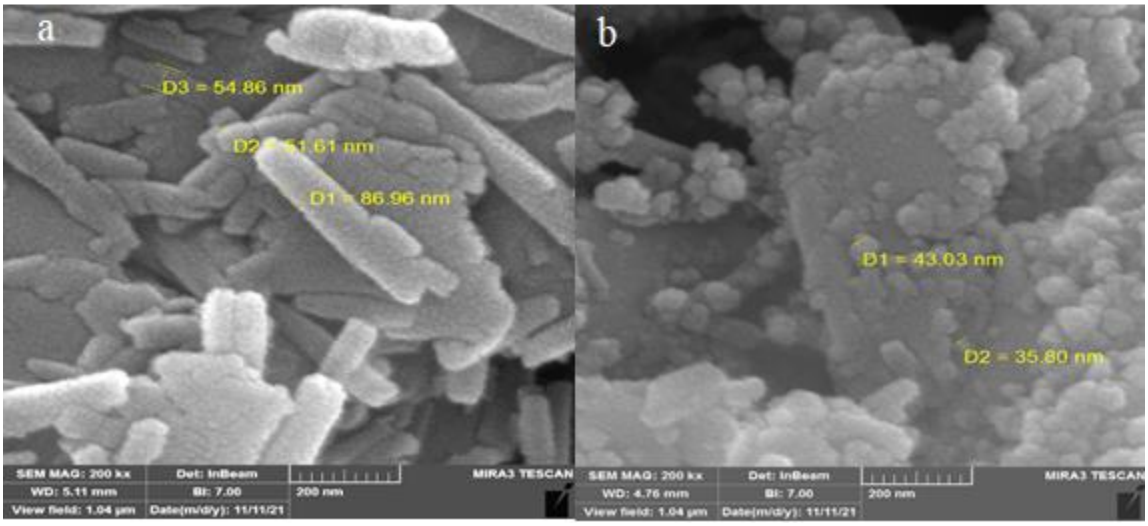

Figure 1. SEM images of kaolin and the Fe_2O_3–Kaolin

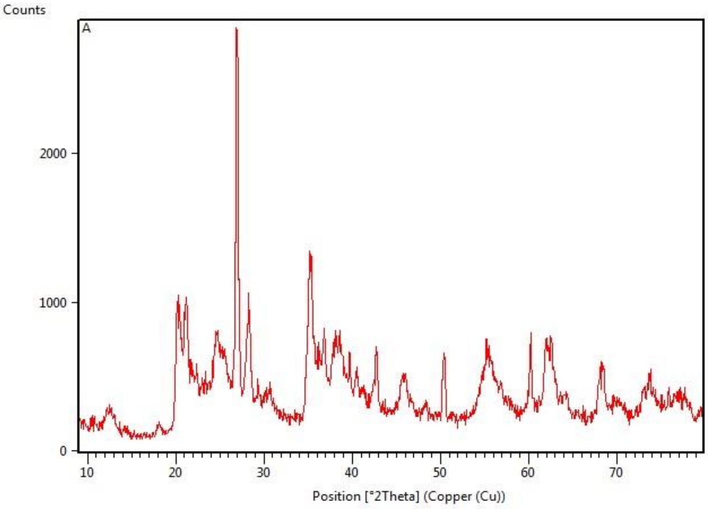

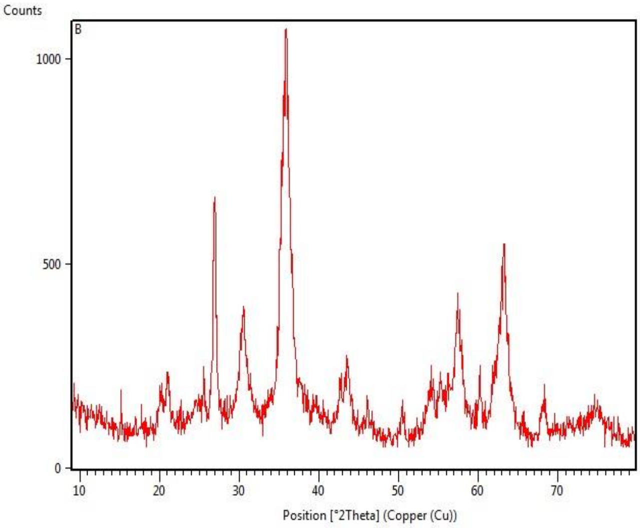

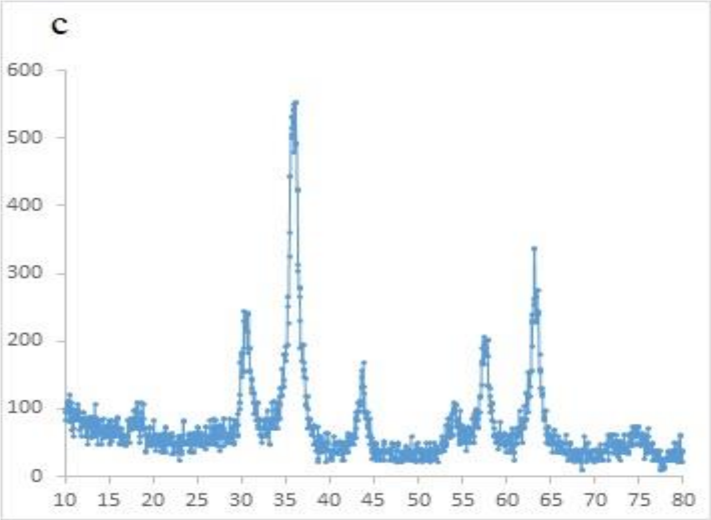

Figure 2. XRD patterns of Kaolin, Fe_2O_3–Kaolin, and Fe_2O_3

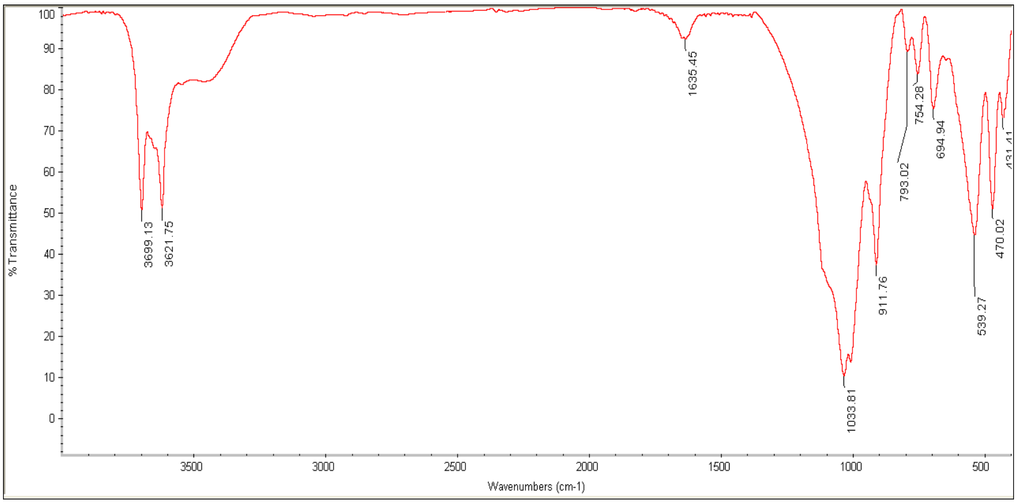

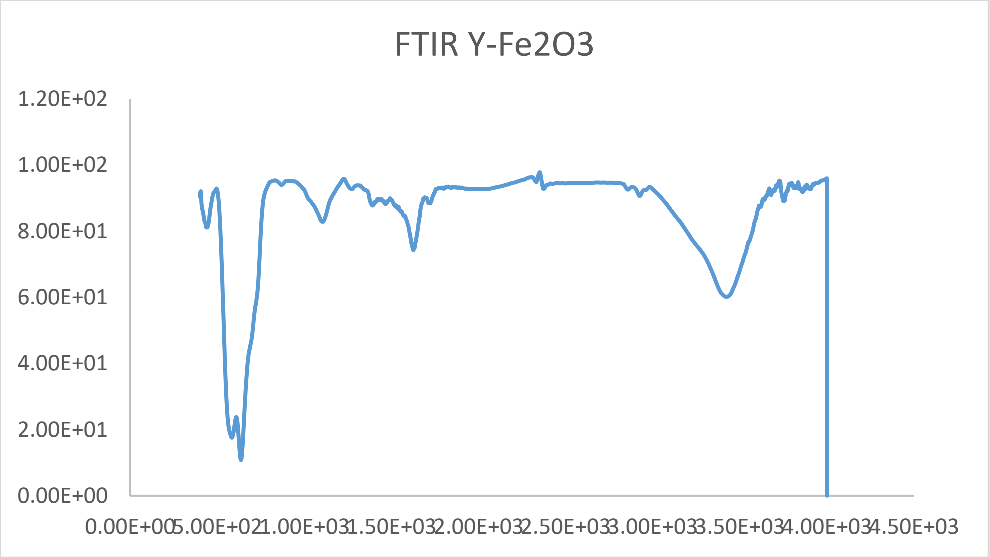

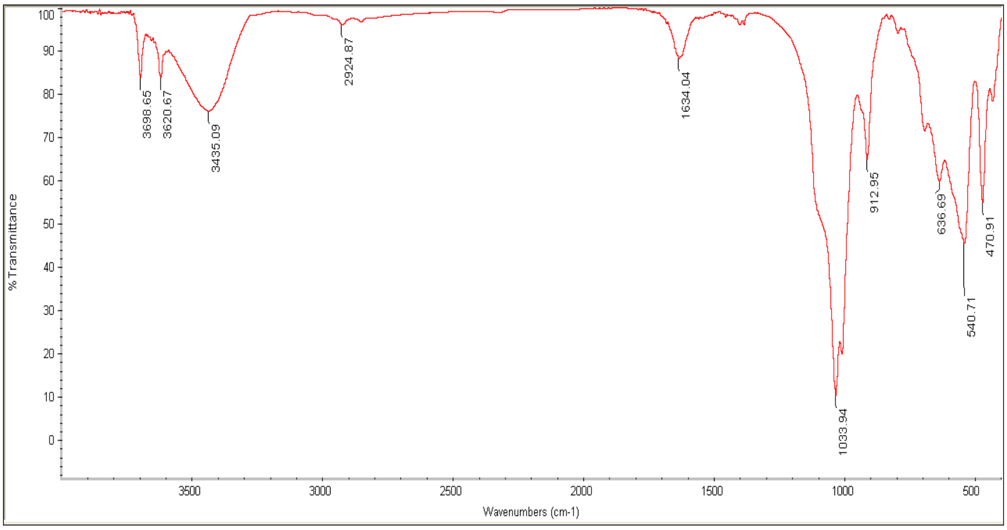

Figure 3. FT-IR spectrum of the Kaolin, Fe_2O_3, and Fe_2O_3–Kaolin

Investigation of pH on removal efficiency

The pH of the solution can play a major role in the adsorption process of a molecule because changes in pH can cause changes in adsorbent and adsorbate charges (35). In the present study, one of the important aspects of antibiotic uptake is the determination of pH_{pzc}. Measuring pH_{pzc} can provide information on the charge and charge distribution on the surface of nanocomposites. This study determined pHpzc to be 6.5, where the adsorbent charge is neutral. The adsorbent surface charge is positive at pH less than pH_{pzc}, while its surface is negatively charged in solutions with pH above pHpzc (36). Thus, as shown in Figures 4a and b, changes in the percentage of removal at different pH values indicate that acidic pH values are more effective in removing both antibiotics; the reason for the mentioned event may be that in acidic pH values, adsorbents have a positive charge and negatively charged ions are better absorbed.

Investigation of initial antibiotic concentration and contact time on removal rate

Changes in the initial concentration of adsorbed pollutants are other factors that affect these systems' adsorption rate. Based on the findings of this study, shown in Figures 5a and b, the removal efficiency increased with increasing the initial concentration of antibiotics from 5 to 20 mg/L. The increase in efficiency with increasing concentration could be stated as the availability of the contaminant and the reduction of the distance between the contaminant and the adsorbent so that the contact between the contaminant and the adsorbent increases (37).

However, the removal efficiency decreased with increasing concentrations from 20 to 120 mg/L. The cause of this phenomenon depends on the number of available contaminant molecules and the active surface at which adsorption occurs; so that, for a constant mass of the adsorbent, the amount of accessible active surface for adsorption remains constant. In this condition, with increasing the initial concentration, the number of contaminant molecules in the adsorption reaction medium increases, which, due to a limited number of adsorption sites, leads to reduced process efficiency (32, 38). Since, in this study, a constant adsorbent mass was considered, and the concentration of contaminants was increased from 20 to 120 mg/L, the ratio of the number of contaminant molecules to the available surface has increased, resulting in reduced adsorption efficiency.

As shown in Figures 6a and b, in the beginning, the rate of antibiotic adsorption by nanocomposites is very high, so the highest removal percentage occurs in the first 15 minutes. Over time and reaching the time of 30 min, the efficiency increased at a slower rate, and after 30 min, the amount of adsorption remained almost constant at some concentrations. Perhaps the cause of this phenomenon can be related to the completion of the adsorption capacity of the adsorbent studied; with the saturation of the adsorbent, the antibiotic adsorption rate from the solution is reduced, the solid and liquid phases reach almost equilibrium, and the rate of antibiotic adsorption to the nanocomposite surface and the rate of ion return from the surface of the adsorbent particles into the solution are equalised (39-41).

Investigation of adsorbent dose

Due to the fact that adsorption is a surface process, the adsorbent mass and the amount of surface available for adsorption have a significant effect on the adsorption efficiency (42). Therefore, the effect of adsorbent concentration on the removal of ceftriaxone and Cefixime antibiotics was investigated. By increasing the adsorbent dose from 0.1 g to 0.4 g at 250 cc, the removal efficiency increased, which could be due to the increase in the number of sites available for antibiotic adsorption. By increasing the adsorbent dose from 0.4 g to 0.5 g in 250 cc, the adsorption efficiency decreases; the reason for the lack of increase in the adsorption of antibiotics for adsorbent doses more than 0.4 g can be the overlap of adsorption sites on the adsorbent surface, which leads to reduction of adsorption sites and thus reduction of efficiency and amount of adsorption (43, 44).

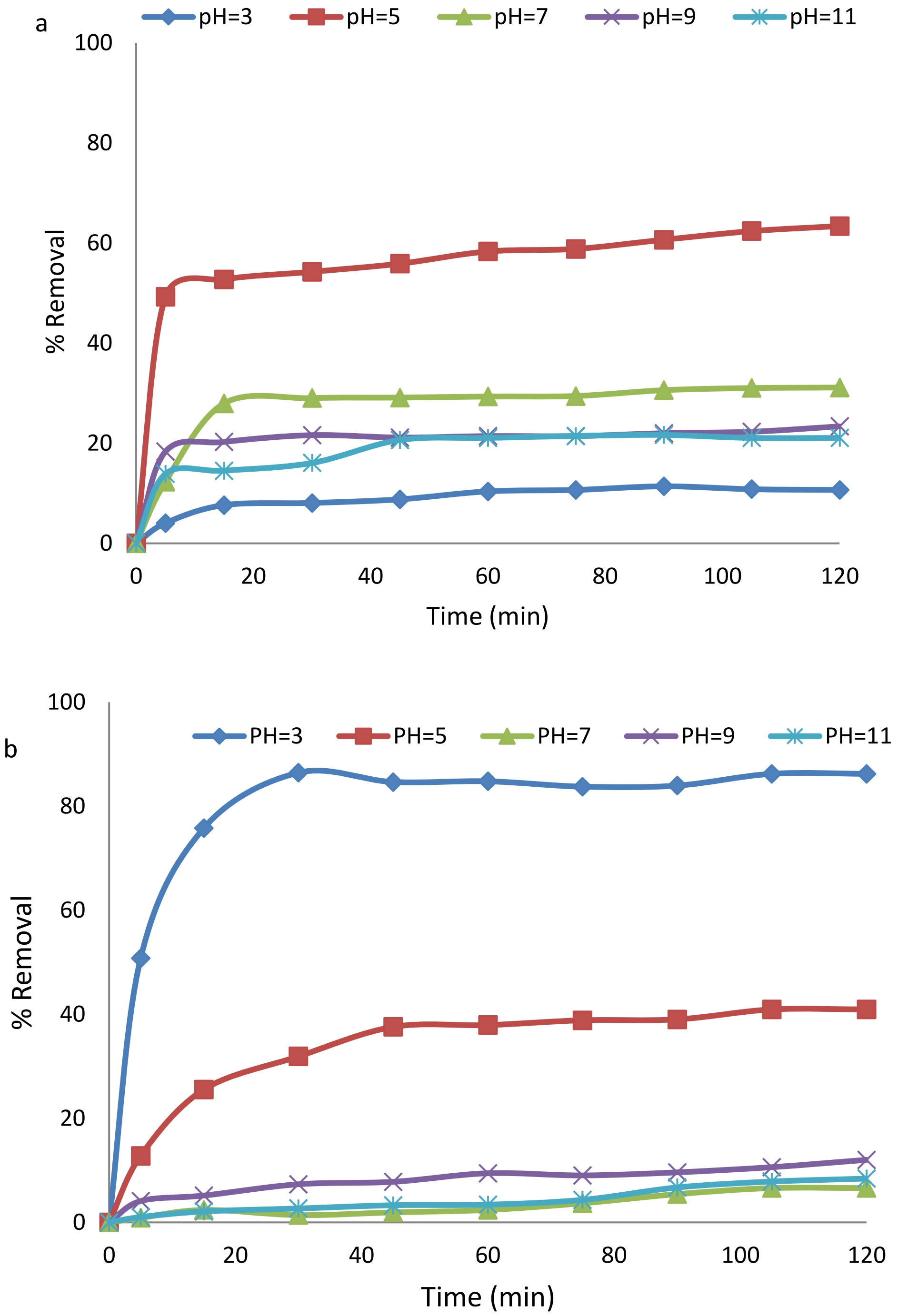

Figure 4. pH study on the rate of antibiotic removal a: Ceftriaxone antibiotic b: Cefixime antibiotic (antibiotic concentrations=20 mg/L, Kaolin-Fe_3O_4 dosage= 0.4 g, contact time=0 to 120, temperature=25C°)

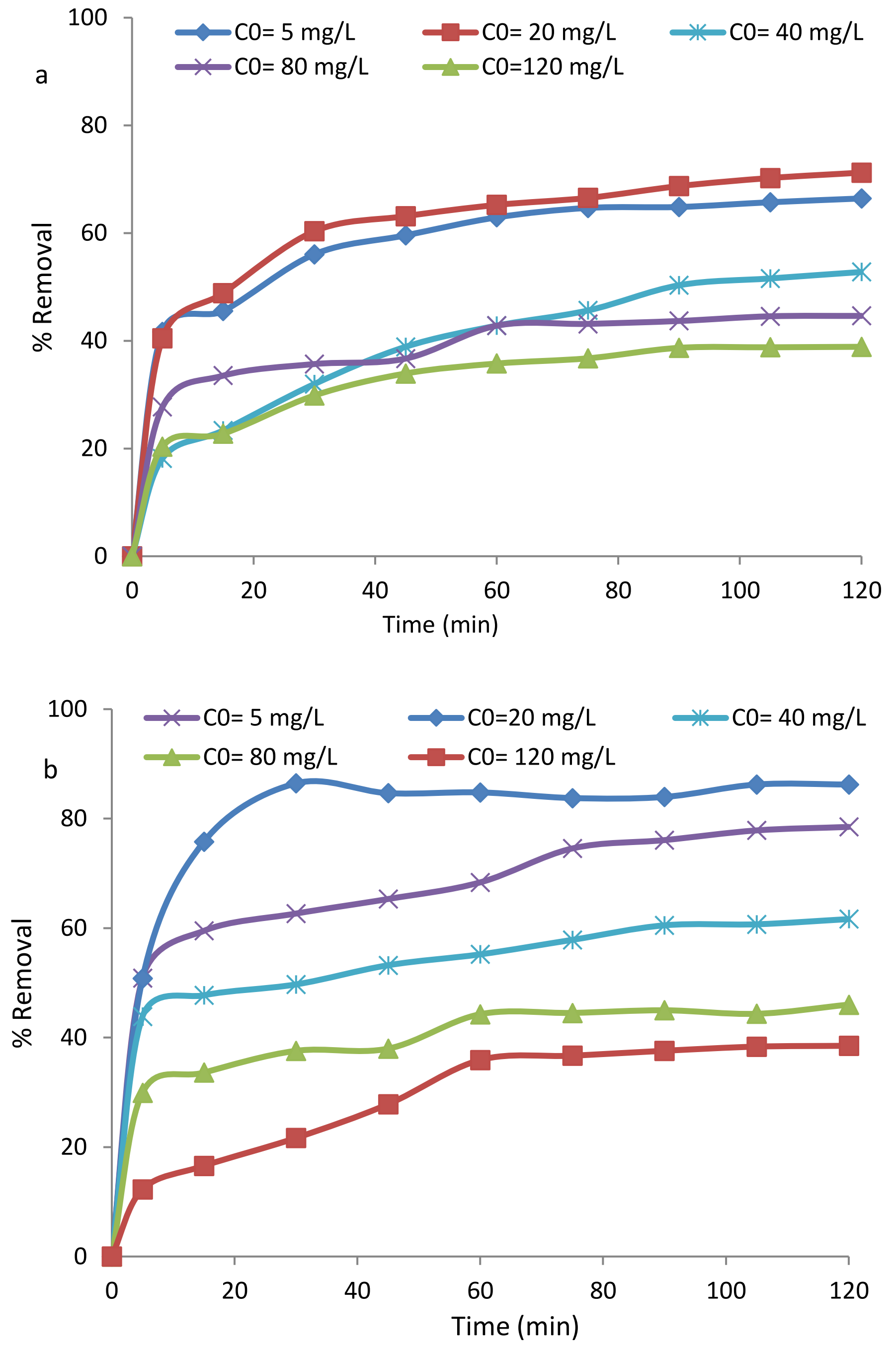

Figure 5. Evaluation of concentration and contact time on the antibiotic removal rate:

A) Ceftriaxone antibiotic (Kaolin-Fe_3O_4 dosage= 0.4 g, pH= 5, and temperature=25C°)

B) Cefixime antibiotic (Kaolin-Fe_3O_4 dosage= 0.4 g, pH= 3, and temperature=35C°)

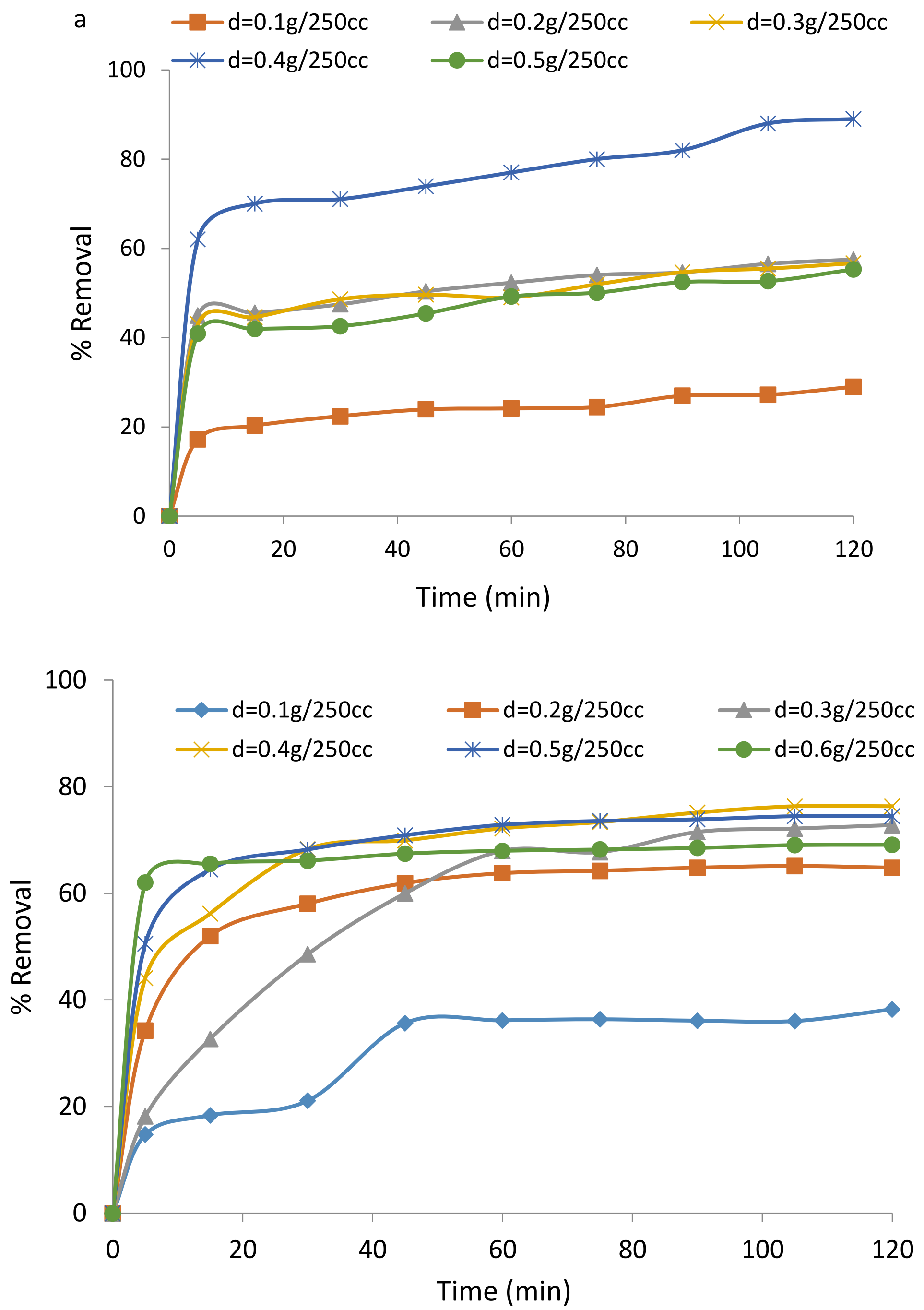

Figure 6. Evaluation of nanocomposite dose on antibiotic removal rate:

A) Ceftriaxone antibiotic (antibiotic concentrations=20 mg/L, pH=5, contact time=0 to 120, and temperature=25C°)

B) Cefixime antibiotic (antibiotic concentrations=20 mg/L, pH=3, contact time=0 to 120, and temperature=35C°)

Adsorption isotherm and kinetics

To understand the mechanism of contaminant adsorption on the nanocomposite, it is necessary to perform experiments related to adsorption kinetics and isotherms. In this study, to understand the mechanism of adsorption, PFO and PSO and Elovich and intraparticle diffusion were used. In these equations, q_e and qt are the adsorption capacity in the equilibrium and time t, respectively. The constant K1 and K2 correspond to the PFO in terms of (1/min) and (g/mg. min). α represents the initial adsorption rate (mg/g min), while β is the extent of surface coverage (g/mg) and the process activation energy. ki is a constant rate of intraparticle diffusion (g/mg min), and C, reflects the effect of the boundary layer or adsorption.

Adsorption isotherms are graphical representations of the adsorbed particle behaviour on the surface of a solid or liquid. By looking at this isotherm, we can get an idea of how the adsorption process works and, therefore, what are the particle-surface interactions and surface properties. By analysing the isotherm, a smooth, porous, or finely porous surface is obtained. For studying how to connect and adsorb pollutants, two parametric isotherm models, including Langmuir, Freundlich, and Temkin, and three parametric isotherm models, including Redlich-Peterson and sips, were used, and then their equations were given in Table 1.

In addition to the regression coefficient, the RMSE error coefficient was used to ensure the correctness of matching, which is defined as follows (45):

Residual Root Mean Square Error (RMSE)=

$$\sqrt{\left(\frac{1}{n-1}\sum_{i=1}^{n}(q_{e,exp} - q_{e,cal})\right)^2} \qquad (3)$$

where q_e exp and q_e cal are equal to the experimental and calculated adsorption capacity, and n is the number of relevant experiments.

The results for the kinetic calculations are shown in Tables 2 and 3; as can see in Table 2, the equilibrium data follow all three first- and second-order kinetics and Elovich according to the regression coefficient. The error coefficient is low for all three mentioned kinetics. The study of q_e exp and q_e cal also confirms that the equilibrium data follow all three kinetics so that the q_e exp and q_e cal were close to each other. Furthermore, for the intraparticle diffusion kinetics, the regression coefficient was higher, and the error coefficient was lower, indicating the compliance of data with this kinetic model. The study of this model showed that the adsorption mechanism consists of one step, i.e., the occurrence of adsorption only on the adsorbent surface. With increasing concentration, both C and K coefficients increase, indicating adsorbent's tendency to absorb high concentrations of antibiotics.

Table 3 also shows the adsorption kinetics for ceftriaxone. As can be seen, the equilibrium data of all pseudo-first-order kinetic (PFO) and pseudo-second-order kinetic (PSO) and Elovich and intraparticle diffusion are fixed. The regression coefficient for all of them is higher than 0.9 at all concentrations, except for two cases (for concentrations of 5 mg/L, the regression coefficient for PFO and PSO was less than 0.9). However, in general, by considering all the parameters and considering that the error coefficient for Elovich kinetics was less than one, we can say that the equilibrium data follow this model more. When kinetic data were analysed using the intraparticle diffusion model for both antibiotics, it was observed that the diagram does not cross the origin, indicating that the intraparticle diffusion is not the only rate-limiting step.

In isotherm studies, C_e is equilibrium concentration (mg/L), q_e is indicative of the amount of adsorbed material (mg/g), q_m represents a maximum amount of adsorbed ions per unit of adsorbent mass (maximum adsorption capacity (mg/g), k_L is equilibrium constant (lit/mg). R_L is the Langmuir separation factor. In this concept, the lower values of RL represent the adsorbent's better adsorption. The values of R_L show whether the adsorption process is irreversible (R_L= 0), linear (R_L= 1), favorable ($0<R_L<1$) or undesirable ($R_L>1$) (46).

K_f and n are Freundlich constants where K_f is the correlation of the amount of antibiotic absorbed in the adsorbent per unit equilibrium, and n indicates the desired amount of adsorption process. Moreover, B is Temkin isotherm constant (kJ/mole), and K_T is the binding constant, representing the maximum binding energy (lit/gr).

The slope of the linear equation of Freundlich isotherm (1/n) varies between zero and 1, a measure of surface adsorption intensity and surface heterogeneity. With increasing heterogeneity intensity, this value approaches zero.

Sips isotherm is a combination of Langmuir and Freundlich models that are used to predict heterogeneous adsorption systems and remove the limitations of the Freundlich model. This model has converted to Freundlich isotherm at low concentrations of adsorbate, while at high concentrations, it predicts the specific monolayer adsorption capacity of the Langmuir isotherm.

The Sips isotherm equation is characterised by a dimensionless heterogeneity coefficient (n), which can also describe system heterogeneity between 0 and 1. When n=1, the Sips equation is reduced to the Langmuir equation and means homogeneous absorption.

The K_R constant is the Redlich-Peterson adsorption capacity, which is determined by trial and error to obtain the maximum linear regression value of the isotherm diagram. This parameter is R-P isotherm constant and is between 0 and 1. Moreover, when the aR is equal to one, the R-P equation becomes the Langmuir isotherm equation, and when the aR equals zero, it is closer to the Freundlich equation.

The results of isotherms are shown in Table 4 and Figure 6; as can be seen, Freundlich and Sips isotherms with high regression coefficient and lower error coefficient have a high agreement with the equilibrium data. Also, the value of RL in this equation is equal to 0.17 for Cefixime adsorption and 0.22 for ceftriaxone absorption, which is between zero and one, which is very desirable for adsorption. Furthermore, the value of 1/n is equal to 0.552 for ceftriaxone adsorption and is equal to 0.393 for Cefixime uptake, which is between zero and one, which indicates the optimal adsorption of both antibiotics by the Freundlich isotherm. The aR value for both antibiotics also tends to be zero, indicating adaptation to the Freundlich isotherm.

Table 1. Non-linear forms of kinetic and isotherms models

Models	Non-lineair Forms	Ref.
	Kinetic models	
PFO	$q_t = q_e(1 - e^{-k_1 t})$	[29]
PSO	$q_t = \frac{k_2 q_e^2 t}{1 + k_2 q_e t}$	[30]
Elovich	$q_t = \frac{\ln(\alpha\beta)}{\beta} + \frac{\ln(t)}{\beta}$	[34]
IPD	$q_t = K_{id} t^{1/2}$+C	[35]
	Two-Parameter isotherms	
Langmuir	$\mathrm{Q_e} = \frac{Q_m K_L \mathrm{C_e}}{1 + K_L \mathrm{C_e}}$	[36]
Freundlich	$\mathrm{Q_e}=\mathrm{K_F Ce}^{1/n}$	[37]
Temkin	$Q_e = \frac{RT}{\Delta Q} ln(A_T C_e)$	[38]
Redlich-Peterson	$\mathrm{Q_e} = \frac{A\mathrm{C_e}}{1 + \mathrm{B}C_e^{\beta}}$	[39]
Sips	$\mathrm{Q_e} = \frac{K_s C_e^{\beta}}{1 + a_s C_e^{\beta s}}$	[40]

Table 2. Kinetic data obtained by non-linear fitting analysis for Cefixime adsorption

Kinetic model	Parameter	Cefixime (mg/L)				
		5	20	40	80	120
	q_{max} experiment (mg/g)	2.45	10.77	15.41	23.00	28.90
pseudo-first-order (PFO)	q_{max} (mg/g)	2.34	10.62	14.11	21.25	30.52
	K_1 (L mg^{-1})	0.098	0.174	0.283	0.208	0.029
	R^2	0.735	0.999	0.993	0.992	0.892
	RMSE	0.258	0.177	1.07	1.79	2.79
pseudo-second-order (PSO)	q_{max} (mg/ g)	2.34	11.22	15.36	23.39	36.62
	K_2 (L/ mg)	0.098	0.026	0.017	0.008	0.0009
	R^2	0.735	0.940	0.792	0.846	0.909
	RMSE	0.258	0.309	0.904	1.32	2.32
Elovich	q_{max} (mg/ g)	2.43	11.66	15.23	23.12	29.23
	α	0.291	1.58	1.57	2.87	6.79
	β (L/ mg)	35.05	12.90	135.1	25.73	0.614
	R^2	0.952	0.806	0.941	0.941	0.917
	RMSE	0.06	0.726	0.368	0.674	1.90
Intra particle diffusion	q_{max} (mg/ g)	2.50	12.43	15.61	23.93	30.67
	Ki	0.101	0.648	0.538	1.018	2.25
	C	1.396	5.325	9.70	12.78	6.01
	R^2	0.979	0.697	0.989	0.934	0.995
	RMSE	0.039	1.13	0.15	0.714	1.20

Table 3. Kinetic data obtained by non-linear fitting analysis for Ceftriaxone adsorption

Kinetic model	Parameter	Ceftriaxone (mg/L)				
		5	20	40	80	120
	q_{max} experiment (mg/g)	2.07	8.90	13.19	22.31	29.16
pseudo-first-order (PFO)	q_{max} (mg/g)	2.03	8.31	12.45	20.75	28.92
	K_L (L mg^{-1})	0.089	0.136	0.042	0.186	0.058
	R^2	0.805	0.994	0.978	0.992	0.948
	RMSE	0.193	0.584	1.47	1.72	1.55
pseudo-second-order (PSO)	q_{max} (mg/ g)	2.14	9.05	16.15	22.87	31.62
	K_2 (L/ mg)	0.088	0.020	0.002	0.008	0.003
	R^2	0.894	0.942	0.955	0.867	0.977
	RMSE	0.101	0.315	0.70	1.22	0.841
Elovich	q_{max} (mg/ g)	2.12	8.99	12.76	22.61	30.36
	α	0.280	1.259	2.792	2.96	5.98
	β (L/ mg)	16.02	10.52	0.803	17.18	1.32
	R^2	0.965	0.986	0.952	0.953	0.987
	RMSE	0.049	0.141	0.583	0.612	0.628
Intra particle	q_{max} (mg/ g)	2.20	9.40	13.82	23.46	31.82
	Ki	0.1009	0.458	1.06	1.05	2.02
	C	1.09	4.37	2.11	11.94	9.68
	R^2	0.927	0.928	0.988	0.942	0.993
	RMSE	0.074	0.338	0.314	0.688	1.61

Table 4. isotherm data obtained by non-linear fitting analysis for Cefixime and Ceftriaxone adsorption

Isotherm	Parameters	Ceftriaxone	Cefixime
Experiment	q_{max} (mg/ g)	29.17	28.87
Langmuir	q_{max} (mg/ g)	28.23	26.48
	K_L (L mg^{-1})	0.028	0.102
	R^2	0.981	.950
	RMSE	1.61	2.60
Freundlich	q_{max} (mg/ g)	29.22	28.79
	1/n	0.552	0.393
	K_F (L mg^{-1})	2.72	5.29
	R^2	0.991	0.974
	RMSE	1.08	1.86
Temkin	q_{max} (mg/ g)	26.81	26.84
	B	440.3	440.3
	K_T (L mg^{-1})	1.6	1.6
	R^2	0.943	0.958
	RMSE	3.73	1.88
Sips	q_{max} (mg/ g)	29.11	28.41
	k_L	2.60	5.20
	n	0.587	0.475
	a_R	0.009	0.054
	R^2	0.989	0.975
	RMSE	1.08	1.84
Redlich- Peterson	q_{max} (mg/ g)	29.23	28.80
	K_R/(L g^{-1})	2922	3017
	a_R/(L $mmol^{-1}$)	10.72	570.0
	g	0.448	0.606
	R^2	0.990	0.974
	RMSE	1.40	1.86

Determination of thermodynamic parameters

One of the most important parameters in the pollutant adsorption process is the temperature to understand how the pollutant is absorbed at different temperatures. Therefore, it is very important to determine thermodynamic parameters. Thermodynamic parameters, including standard Gibb's free energy (ΔG^0), standard enthalpy (ΔH^0), and standard entropy (ΔS^0) can be calculated using the following Eqs (47).

$$K_d = q_e/C_e \qquad (4)$$

$$\mathrm{Ln}\,(K_d) = \frac{\Delta S^0}{R} - \frac{\Delta H^0}{RT} \qquad (5)$$

$$\Delta G^0 = \Delta H - T\,\Delta S^0 \qquad (6)$$

By plotting the van't hoff diagram, i.e., ln K_d against 1/T, and obtaining the line equation, the values of ΔH^0 and ΔS^0 can be extracted using slope and intercept, respectively. Then, using the equations, the ΔG^0 can be calculated at the desired temperatures.

The results of thermodynamic parameters for the adsorption of both antibiotics are shown in Table 5, and as can be seen, the negative ΔG^0 indicate that the adsorption process is spontaneous (48). The increase in ΔG^0 with increasing temperature indicates a decrease in the rate of spontaneous reactions at higher temperatures; or in other words, lower temperatures are more desirable for the absorption of both antibiotics (45). It should be noted that the positive ΔH^0 changes of reaction indicate that the adsorption process is exothermic. On the other hand, the positive ΔS^0 for the adsorption of both standard antibiotics in the system indicates an increase in irregularities in the solid/solution adsorption interface (49). In other words, the positive ΔS^0 of the system indicates an increase in irregularities in the nanocomposite in the adsorption process of antibiotic ions compared to the initial state before the adsorption process. Due to this, it can be suggested that changes and increases in irregularities in the nanocomposite structure occur during the adsorption process (50, 51).

Table 5. Thermodynamic parameters for the adsorption of Cefixime and ceftriaxone on nanocomposites

T (K)	ΔG^0 (kJ/mol)	ΔH^0 (kJ/mol)	ΔS^0 (kJ/mol K)
		Cefixime	
298	−0.851	-3/70	0.011
308	−0.623		
318	−0.319		
328	-0.121		
		ceftriaxone	
298	−1.17	-3/40	0/009
308	−0.782		
318	−0.532		
328	-0.379		

Conclusion

Kaolin-Fe_3O_4 magnetic nanocomposite was prepared by simple chemical and physical methods, and aqueous solutions were used to remove ceftriaxone and Cefixime ions. Adsorbent properties were determined by SEM, FTIR analysis, pH_{pzc}, and XRD. In addition, the study of various factors affecting the removal of antibiotics by Kaolin-Fe_3O_4 nanocomposite was considered. Increasing the Kaolin-Fe_3O_4 mass was associated with increasing the adsorption efficiency, and the highest removal percentage was obtained using 0.4 g in 250 cc of adsorbent. In addition, studies evaluating the effect of adsorption time introduced 60 minutes as the adsorption equilibrium time. Fitting the data with different kinetics used to perform kinetic studies confirmed the suitability of different models for the adsorption data. The Freundlich and Sips model best fitted isotherm data. Thermodynamic studies were performed by calculating different thermodynamic parameters. According to the results, the removal process of ceftriaxone and Cefixime by the studied adsorbent, i.e., Kaolin-Fe_3O_4 nanocomposite, was a spontaneous and exothermic adsorption process. According to our work, the application of novel Kaolin-Fe_3O_4 magnetic nanocomposite could contribute to the removal of such challenging and persistent contaminants from wastewater.

Acknowledgments

The support of the Research Vice-Chancellor of Guilan University of Medical Sciences is wholeheartedly appreciated.

References

1. Shakeria E, Mousazadeha M, Ahmadparic H, Kabdaşlıd I, Ali H, Jamalie NSG, et al. Electrocoagulation-flotation treatment followed by sedimentation of carpet cleaning wastewater: optimisation of key operating parameters via RSM-CCD. DESALINATION AND WATER TREATMENT. 2021;227:163-76.
2. Anggraini M, Kurniawan A, Ong LK, Martin MA, Liu J-C, Soetaredjo FE, et al. Antibiotic detoxification from synthetic and real effluents using a novel MTAB surfactant-montmorillonite (organoclay) sorbent. RSC advances. 2014;4(31):16298-311.
3. Nairi V, Medda L, Monduzzi M, Salis A. Adsorption and release of ampicillin antibiotic from ordered mesoporous silica. Journal of Colloid and Interface Science. 2017;497:217-25.
4. Doroudi Z, Jalali Sarvestani MR. Boron nitride nanocone as an adsorbent and senor for Ampicillin: a computational study. Chemical Review and Letters. 2020;3(3):110-6.
5. Erşan M, Bağda E, Bağda E. Investigation of kinetic and thermodynamic characteristics of removal of tetracycline with sponge like, tannin based cryogels. Colloids and surfaces B: Biointerfaces. 2013;104:75-82.
6. Abukhadra MR, Helmy A, Sharaf MF, El-Meligy MA, Soliman ATA. Instantaneous oxidation of levofloxacin as toxic pharmaceutical residuals in water using clay nanotubes decorated by ZnO (ZnO/KNTs) as a novel photocatalyst under visible light source. Journal of Environmental Management. 2020;271:111019.
7. Al-Jabari MH, Sulaiman S, Ali S, Barakat R, Mubarak A, Khan SA. Adsorption study of levofloxacin on reusable magnetic nanoparticles: Kinetics and antibacterial activity. Journal of Molecular Liquids. 2019;291:111249.
8. Antonelli R, Malpass GRP, da Silva MGC, Vieira MGA. Adsorption of ciprofloxacin onto thermally modified bentonite clay: Experimental design, characterisation, and adsorbent regeneration. Journal of Environmental Chemical Engineering. 2020;8(6):104553.
9. Khodadadi M, Panahi AH, Al-Musawi TJ, Ehrampoush M, Mahvi A. The catalytic activity of FeNi3@ SiO2 magnetic nanoparticles for the degradation of tetracycline in the heterogeneous Fenton-like treatment method. Journal of Water Process Engineering. 2019;32:100943.
10. Zhao Y, Wang Y, Liu E, Fan J, Hu X. Bi2WO6 nanoflowers: an efficient visible light photocatalytic activity for ceftriaxone sodium degradation. Applied Surface Science. 2018;436:854-64.
11. Wen Q, Kong F, Zheng H, Yin J, Cao D, Ren Y, et al. Simultaneous processes of electricity generation and ceftriaxone sodium degradation in an air-cathode single chamber microbial fuel cell. Journal of Power Sources. 2011;196(5):2567-72.
12. Zhao Y, Liang X, Wang Y, Shi H, Liu E, Fan J, et al. Degradation and removal of Ceftriaxone sodium in aquatic environment with Bi2WO6/g-C3N4 photocatalyst. Journal of colloid and interface science. 2018;523:7-17.
13. Azarpira H, Balarak D. Rice husk as a biosorbent for antibiotic metronidazole removal: isotherm studies and model validation. International Journal of ChemTech Research. 2016;9(7):566-73.
14. Chaturvedi G, Kaur A, Umar A, Khan MA, Algarni H, Kansal SK. Removal of fluoroquinolone drug, levofloxacin, from aqueous phase over iron based MOFs, MIL-100 (Fe). Journal of Solid State Chemistry. 2020;281:121029.
15. Chen C-H, Lin Y-C, Peng Y-P, Lin M-H. Simultaneous hydrogen production and ibuprofen degradation by green synthesised Cu2O/TNTAs photoanode. Chemosphere. 2021;284:131360.
16. Fan G, Yang S, Du B, Luo J, Lin X, Li X. Sono-photo hybrid process for the synergistic degradation of levofloxacin by FeVO4/BiVO4: Mechanisms and kinetics. Environmental Research. 2022;204:112032.
17. He W, Li Z, Lv S, Niu M, Zhou W, Li J, et al. Facile synthesis of Fe3O4@ MIL-100 (Fe) towards enhancing photo-Fenton like degradation of levofloxacin via a synergistic effect between Fe3O4 and MIL-100 (Fe). Chemical Engineering Journal. 2021;409:128274.

18. Mousazadeh M, Niaragh EK, Usman M, Khan SU, Sandoval MA, Al-Qodah Z, et al. A critical review of state-of-the-art electrocoagulation technique applied to COD-rich industrial wastewaters. Environmental Science and Pollution Research. 2021;28(32):43143-72.

19. Balarak D, Baniasadi M, Lee S-M, Shim MJ. Ciprofloxacin adsorption onto Azolla filiculoides activated carbon from aqueous solutions. Desal Water Treat. 2021;218:444-53.

20. Huang L, Wang M, Shi C, Huang J, Zhang B. Adsorption of tetracycline and ciprofloxacin on activated carbon prepared from lignin with H3PO4 activation. Desalination and Water Treatment. 2014;52(13-15):2678-87.

21. Mousazadeh M, Naghdali Z, Al-Qodah Z, Alizadeh S, Niaragh EK, Malekmohammadi S, et al. A systematic diagnosis of state of the art in the use of electrocoagulation as a sustainable technology for pollutant treatment: An updated review. Sustainable Energy Technologies and Assessments. 2021;47:101353.

22. Peng X, Hu F, Dai H, Xiong Q, Xu C. Study of the adsorption mechanisms of ciprofloxacin antibiotics onto graphitic ordered mesoporous carbons. Journal of the Taiwan Institute of Chemical Engineers. 2016;65:472-81.

23. Iwuozor KO, Abdullahi TA, Ogunfowora LA, Emenike EC, Oyekunle IP, Gbadamosi FA, et al. Mitigation of levofloxacin from aqueous media by adsorption: a review. Sustainable Water Resources Management. 2021;7(6):1-18.

24. Mustafanejad F, Sajjadi N, Marandi R, Zaeimdar M. Efficient removal of crystal violet by sulphonic-modified multi-walled carbon nanotube and graphene oxide. Nanotechnology for Environmental Engineering. 2021;6(2):1-9.

25. Mouni L, Belkhiri L, Bollinger J-C, Bouzaza A, Assadi A, Tirri A, et al. Removal of Methylene Blue from aqueous solutions by adsorption on Kaolin: Kinetic and equilibrium studies. Applied Clay Science. 2018;153:38-45.

26. Namvar-Mahboub M. Methylene Blue Removal from Aqueous Solution Using Zein-Modified Kaolin. Journal of Advanced Materials and Technologies. 2020;9(2):53-61.

27. Gao W, Zhao S, Wu H, Deligeer W, Asuha S. Direct acid activation of kaolinite and its effects on the adsorption of methylene blue. Applied Clay Science. 2016;126:98-106.

28. Asrari E. Study of possibility using modified concrete with Kaolin absorbent for removeing heavy metal of Chromium (VI) from wastewater bent. Modares Civil Engineering journal. 2019;18(6):27-37.

29. Yilmaz M, Al-Musawi TJ, Khatibi AD, Baniasadi M, Balarak D. Synthesis of activated carbon from Lemna minor plant and magnetised with iron (III) oxide magnetic nanoparticles and its application in removal of Ciprofloxacin. Biomass Conversion and Biorefinery. 2022:1-14.

30. Al-Musawi TJ, Mengelizadeh N, Taghavi M, Mohebi S, Balarak D. Activated carbon derived from Azolla filiculoides fern: a high-adsorption-capacity adsorbent for residual ampicillin in pharmaceutical wastewater. Biomass conversion and biorefinery. 2021:1-13.

31. Guo S, Zhang G, Wang J. Photo-Fenton degradation of rhodamine B using Fe2O3–Kaolin as heterogeneous catalyst: Characterisation, process optimisation and mechanism. Journal of colloid and interface science. 2014;433:1-8.

32. Wang F, Sun W, Pan W, Xu N. Adsorption of sulfamethoxazole and 17β-estradiol by carbon nanotubes/CoFe2O4 composites. Chemical Engineering Journal. 2015;274:17-29.

33. Carrales-Alvarado DH, Leyva-Ramos R, Rodríguez-Ramos I, Mendoza-Mendoza E, Moral-Rodríguez AE. Adsorption capacity of different types of carbon nanotubes towards metronidazole and dimetridazole antibiotics from aqueous solutions: effect of morphology and surface chemistry. Environmental Science and Pollution Research. 2020;27(14):17123-37.

34. Oliveira LC, Petkowicz DI, Smaniotto A, Pergher SB. Magnetic zeolites: a new adsorbent for removal of metallic contaminants from water. Water research. 2004;38(17):3699-704.

35. Deng Y, Ok YS, Mohan D, Pittman Jr CU, Dou X. Carbamazepine removal from water by carbon dot-modified magnetic carbon nanotubes. Environmental research. 2019;169:434-44.

36. Xiong W, Zeng G, Yang Z, Zhou Y, Zhang C, Cheng M, et al. adsorption of tetracycline antibiotics from aqueous solutions on nanocomposite multi-walled carbon nanotube functionalised MIL-53 (Fe) as new adsorbent. Science of the Total Environment. 2018;627:235-44.

37. Huang Y, Zhu J, Liu H, Wang Z, Zhang X. Preparation of porous graphene/carbon nanotube composite and adsorption mechanism of methylene blue. SN Applied Sciences. 2019;1(1):1-11.

38. Wu Y, Liu W, Wang Y, Hu X, He Z, Chen X, et al. Enhanced removal of antibiotic in wastewater using liquid nitrogen-treated carbon material: material properties and removal mechanisms. International Journal of Environmental Research and Public Health. 2018;15(12):2652.

39. Al-Musawi TJ, Mahvi AH, Khatibi AD, Balarak D. Effective adsorption of ciprofloxacin antibiotic using powdered activated carbon magnetised by iron (III) oxide magnetic nanoparticles. Journal of Porous Materials. 2021;28(3):835-52.

40. Chitongo R, Opeolu BO, Olatunji OS. Abatement of amoxicillin, ampicillin, and chloramphenicol from aqueous solutions using activated carbon prepared from grape slurry. CLEAN–Soil, Air, Water. 2019;47(2):1800077.

41. Rahman N, Varshney P. Assessment of ampicillin removal efficiency from aqueous solution by polydopamine/zirconium (IV) iodate: optimisation by response surface methodology. RSC Advances. 2020;10(34):20322-37.

42. Yang H, Liu Q, Masse S, Zhang H, Li L, Coradin T. Hierarchically-organized, well-dispersed hydroxyapatite-coated magnetic carbon with combined organics and inorganics removal properties. Chemical Engineering Journal. 2015;275:152-9.

43. Ahmadi S, Banach A, Mostafapour FK, Balarak D. Study survey of cupric oxide nanoparticles in removal efficiency of ciprofloxacin antibiotic from aqueous solution: adsorption isotherm study. Desalination and water treatment. 2017;89:297-303.

44. Balarak D, Taheri Z, Shim MJ, Lee S-M, Jeon C. Adsorption kinetics and thermodynamics and equilibrium of ibuprofen from aqueous solutions by activated carbon prepared from Lemna minor. Desal Water Treat. 2021;215:183-93.

45. Fakhri A, Rashidi S, Asif M, Tyagi I, Agarwal S, Gupta VK. Dynamic adsorption behavior and mechanism of Cefotaxime, Cefradine and Cefazolin antibiotics on CdS-MWCNT nanocomposites. Journal of Molecular Liquids. 2016;215:269-75.

46. Yu F, Li Y, Han S, Ma J. Adsorptive removal of antibiotics from aqueous solution using carbon materials. Chemosphere. 2016;153:365-85.

47. Ge Y-L, Zhang Y-F, Yang Y, Xie S, Liu Y, Maruyama T, et al. Enhanced adsorption and catalytic degradation of organic dyes by nanometer iron oxide anchored to single-wall carbon nanotubes. Applied Surface Science. 2019;488:813-26.

48. Fei Y, Li Y, Han S, Ma J. Adsorptive removal of ciprofloxacin by sodium alginate/graphene oxide composite beads from aqueous solution. Journal of colloid and interface science. 2016;484:196-204.

49. Shikuku VO, Zanella R, Kowenje CO, Donato FF, Bandeira NM, Prestes OD. Single and binary adsorption of sulfonamide antibiotics onto iron-modified clay: linear and non-linear isotherms, kinetics, thermodynamics, and mechanistic studies. applied water science. 2018;8(6):1-12.

50. Berges J, Moles S, Ormad MP, Mosteo R, Gómez J. Antibiotics removal from aquatic environments: adsorption of enrofloxacin, trimethoprim, sulfadiazine, and amoxicillin on vegetal powdered activated carbon. Environmental Science and Pollution Research. 2021;28(7):8442-52.

51. Pan M. Biochar adsorption of antibiotics and its implications to remediation of contaminated soil. Water, Air, & Soil Pollution. 2020;231(5):1-15.